# Separation and Tracking of Multiple Broadband Sources with One Electromagnetic Vector Sensor

**A structure for adaptively separating, enhancing and tracking uncorrelated sources with an electromagnetic vector sensor (EMVS) is presented. The structure consists of a set of parallel spatial processors, one for each individual source. Two stages of processing are involved in each spatial processor. The first preprocessing stage rejects all other sources except the one of interest, while the second stage is an adaptive one for maximizing the signal-to-noise ratio (SNR) and tracking the desired source. The preprocessings are designed using the latest source parameter estimates obtained from the source trackers, and a redesign is activated periodically or whenever any source has been detected by the source trackers to have made significant movement. Compared with conventional adaptive beamforming, the algorithm has the advantage that no a priori information on any desired signal location is needed, the sources are separated at maximum SNR, and their locations are available. The structure is also well suited for parallel implementation. Numerical examples are included to illustrate the capability and performance of the algorithm.**

## I. INTRODUCTION

In recent years, systems based on the use of electromagnetic vector sensor (EMVS) to estimate unknown source directions and eliminate unknown interferences have received a lot of interests [1–14]. Such sensors are capable of measuring all six components of the electric and magnetic fields at a particular position, and they have the advantage of occupying very little space, being able to make use of polarization and independent of signal frequency.

The use of EMVS for source location was proposed by Nehorai and Paldi [1], following which a number of investigations on the number and type of sources that can be identified have been made [3]. In particular, it was found that one EMVS is able to determine the location and polarization of up to three broadband sources [4]. Recently, the use of minimum noise variance beamforming on an EMVS was studied [5], a cross-product algorithm was investigated for tracking a broadband source based on the Poynting vector [6], and a number of ESPRIT-based algorithms have been investigated for estimating narrowband sources [11–14]. Specifically, some preliminary localization tests with the EMVS manufactured by Flam and Russell, Inc., have also been made by Lincoln Lab at the Massachusetts Institute of Technology, Cambridge [7].

Extending the concept of a 2-stage processing for separating narrowband sources in [14, 15], this paper proposes a structure for adaptively separating, enhancing and tracking up to three uncorrelated broadband sources with an EMVS. The structure consists of a set of parallel spatial processors, one for each individual source. Two stages of processing are involved in each spatial processor. The first preprocessing stage rejects all other sources except the one of interest, while the second stage is an adaptive one for maximizing the signal-to-noise ratio (SNR) and tracking the desired source. A redesign of the preprocessing is activated whenever any source has been detected by the source trackers to have made significant movement. The algorithm has the advantage that no a priori information on any desired signal location is needed, and the sources are separated at maximum SNR. Numerical examples are included to illustrate the capability and performance of the algorithm.

## II. EMVS AND ENVIRONMENT

Fig. 1 shows an example of an EMVS [1] which is able to give a complete vector measurement of the 3 electric and 3 magnetic fields of the electromagnetic waves in the environment. Following the methodology developed in [14, 15], the response of such a sensor to a far-field polarized narrowband signal (say the $n$th one) with a spatial parameter vector of

$$\boldsymbol{\theta}_n = \begin{bmatrix} \phi_n \\ \psi_n \\ \alpha_n \\ \beta_n \end{bmatrix} = \begin{bmatrix} \boldsymbol{\theta}_{n1} \\ \boldsymbol{\theta}_{n2} \\ \boldsymbol{\theta}_{n3} \\ \boldsymbol{\theta}_{n4} \end{bmatrix} = \begin{bmatrix} \text{azimuth} \in (-\pi,\pi] \\ \text{elevation} \in [-\pi/2,\pi/2] \\ \text{polarization orientation} \in (-\pi/2,\pi/2] \\ \text{polarization ellipticity} \in [-\pi/4,\pi/4] \end{bmatrix} \tag{1}$$

can be written as

$$\mathbf{S}(\boldsymbol{\theta}_n) = \begin{bmatrix} -\sin\phi_n & -\cos\phi_n \sin\psi_n \\ \cos\phi_n & -\sin\phi_n \sin\psi_n \\ 0 & \cos\psi_n \\ -\cos\phi_n \sin\psi_n & \sin\phi_n \\ -\sin\phi_n \sin\psi_n & -\cos\phi_n \\ \cos\psi_n & 0 \end{bmatrix} \times \begin{bmatrix} \cos\alpha_n & \sin\alpha_n \\ -\sin\alpha_n & \cos\alpha_n \end{bmatrix} \begin{bmatrix} \cos\beta_n \\ j\sin\beta_n \end{bmatrix}. \tag{2}$$

Manuscript received April 17, 2001; revised March 5 and May 25, 2002; released for publication June 20, 2002.

IEEE Log No. T-AES/38/3/XXXX.

Refereeing of this contribution was handled by L. M. Kaplan.

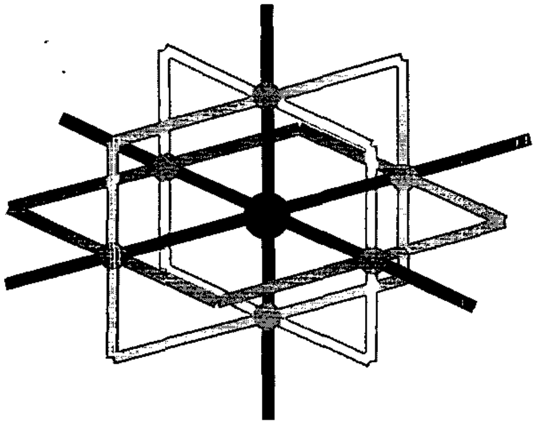

Fig. 1. Example EMVS structure.

The first three components in $\mathbf{S}(\theta_n)$ are the baseband equivalent electric field sensor outputs, while the remaining ones are the outputs from the magnetic field sensors.

As shown in [4], a single EMVS with 6 scalar outputs is able to resolve up to 3 polarized sources. For the purpose of separating and tracking sources, it is assumed without loss of generality that such a sensor is operating in an environment where there are 3 uncorrelated linearly polarized broadband sources with unknown power $\sigma_n^2$ and spatial parameters $(\phi_n, \psi_n, \alpha_n, \beta_n)$, $n = 1, \ldots, 3$. It is also taken for simplicity that appropriate calibration has been made so that the receiver noise in each electric and magnetic sensor has power $\sigma^2$. (The situation of different receiver noise powers in the electric and magnetic sensors can be taken care of by changing the gains of the appropriate amplifiers. The result is equivalent to having the same receiver noise power, but introducing some scaling factors in the components of the space vector.)

In such an environment, the broadband signal received at time $t$ can be written as

$$\mathbf{X}_t = a_{1t}\mathbf{S}(\theta_1) + a_{2t}\mathbf{S}(\theta_2) + a_{3t}\mathbf{S}(\theta_3) + \mathbf{N}_t \qquad (3)$$

where $a_{1t}, \ldots, a_{3t}$ are independent random source signals with powers

$$\mathrm{E}\lfloor |a_n|^2 \rfloor = \sigma_n^2, \qquad n = 1, \ldots, 3 \qquad (4)$$

and $\mathbf{N}_t$ are independent receiver noise with a covariance matrix of

$$\mathrm{E}\lfloor \mathbf{N}_t \mathbf{N}_t^{\mathrm{H}} \rfloor = \sigma^2 \mathbf{I}_6. \qquad (5)$$

## III. OPTIMAL STRUCTURE

Without loss of generality, suppose the first source $\theta_1$ is the desired signal of interest, and the other sources are cochannel interferers. To enhance this source in the presence of possibly much stronger interferences, the EMVS inputs can be linearly combined to result in the output

$$y_{1t} = \mathbf{W}_1^{\mathrm{H}} \mathbf{X}_t \qquad (6)$$

with the weight vector $\mathbf{W}_1$ adjusted to minimize the output power

$$\min_{\mathbf{W}_1} p_{y_1} = \min_{\mathbf{W}_1} \mathrm{E}\lfloor |y_{1t}|^2 \rfloor \qquad (7)$$

while satisfying

$$\mathbf{W}_1^{\mathrm{H}}[\mathbf{S}(\theta_2) \quad \mathbf{S}(\theta_3)] = 0 \qquad (8)$$

and

$$\mathbf{W}_1^{\mathrm{H}} \mathbf{S}(\theta_1) = 1. \qquad (9)$$

Basically, (8) ensures that the interfering sources are rejected, (9) ensures that the response to the desired signal is kept constant, and (7) implies that the noise power is minimized. In other words, this is equivalent to maximizing SNR with a constant response to the desired signal and the interfering sources rejected.

Equations (6)–(9) can be solved in a two-stage process. Firstly, the conditions given by (8) mean that $\mathbf{W}_1 \in C^6$ lie in a subspace $\mathbf{P}_1 \in C^{6\times 4}$ orthogonal to $\mathbf{S}(\theta_2)$ and $\mathbf{S}(\theta_3)$. That is, $\mathbf{W}_1$ can be expressed in terms of a linear combination $\mathbf{W}_{P1} \in C^4$ of the 4 columns of $\mathbf{P}_1$:

$$\mathbf{W}_1 = \mathbf{P}_1^{\mathrm{H}} \mathbf{W}_{P1} \qquad (10)$$

where

$$\mathbf{P}_1^{\mathrm{H}}[\mathbf{S}(\theta_2) \quad \mathbf{S}(\theta_3)] = 0. \qquad (11)$$

As described in the Appendix, $\mathbf{P}_1$ can be determined by using the singular value decomposition of $[\mathbf{S}(\theta_2) \ \mathbf{S}(\theta_3)]$.

From (10) and (11), the problem of (7)–(9) becomes

$$\min_{\mathbf{W}_{P1}} p_{y_1} = \min_{\mathbf{W}_{P1}} \mathrm{E}\lfloor |y_{1t}|^2 \rfloor \qquad (12)$$

subject to

$$\mathbf{W}_{P1}^{\mathrm{H}} \mathbf{S}_{P1}(\theta_1) = 1 \qquad (13)$$

where

$$y_{1t} = \mathbf{W}_{P1}^{\mathrm{H}} \mathbf{X}_{1t} \qquad (14)$$

$$\mathbf{X}_{1t} = \mathbf{P}_1^{\mathrm{H}} \mathbf{X}_t \in C^4 \qquad (15)$$

and

$$\mathbf{S}_{P1}(\theta_1) = \mathbf{P}_1^{\mathrm{H}} \mathbf{S}(\theta_1) \in C^4. \qquad (16)$$

With the introduction of $\mathbf{P}_1$ and using the signal and space vectors $\mathbf{X}_{1t}$ and $\mathbf{S}_{P1}(\theta_1)$ after preprocessing by $\mathbf{P}_1$ the constraint of (8) is removed, and the resulting (12)–(14) is a standard minimum mean square error problem with a linear constraint for preserving the desired signal.

As given in [3], the solution of (12)–(14) is

$$\tilde{\mathbf{W}}_{P1} = \frac{\mathbf{R}_{11}^{-1}\mathbf{S}_{P1}(\theta_1)}{\mathbf{S}_{P1}^{\mathrm{H}}(\theta_1)\mathbf{R}_{11}^{-1}\mathbf{S}_{P1}(\theta_1)} \qquad (17)$$

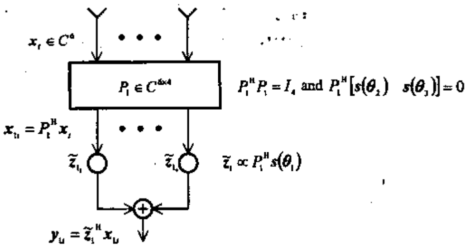


Fig. 2. Optimal processing structure for maximizing SNR for reception of first source while rejecting the other sources.

where $\mathbf{R}_{11}$ is the covariance matrix of $\mathbf{X}_{1t}$ and, from the data model and (14), is given by

$$\mathbf{R}_{11} = \mathrm{E}\lfloor\mathbf{X}_{11}\mathbf{X}_{11}^{\mathrm{H}}\rfloor = \mathbf{P}_1^{\mathrm{H}}\mathrm{E}\lfloor\mathbf{X}_1\mathbf{X}_1^{\mathrm{H}}\rfloor\mathbf{P}_1$$
$$= \sigma_1^2\mathbf{S}_{P1}(\boldsymbol{\theta}_1)\mathbf{S}_{P1}^{\mathrm{H}}(\boldsymbol{\theta}_1) + \sigma^2\mathbf{P}_1^{\mathrm{H}}\mathbf{P}_1. \tag{18}$$

Choosing $\mathbf{P}_1$ to be unitary (the Appendix shows how this can be done in the singular value decomposition process) so that

$$\mathbf{P}_1^{\mathrm{H}}\mathbf{P}_1 = \mathbf{I}_4 \tag{19}$$

the optimal $\mathbf{W}_{P1}$ that maximizes SNR can be easily shown to be simply proportional to

$$\tilde{\mathbf{W}}_{P1} \propto \mathbf{S}_{P1}(\boldsymbol{\theta}_1) = \mathbf{P}_1^{\mathrm{H}}\mathbf{S}(\boldsymbol{\theta}_1). \tag{20}$$

Fig. 2 shows the optimal processing structure based on the above derivation. Also shown are the important equations for the preprocessor $\mathbf{P}_1$ and the optimal weight vector $\tilde{\mathbf{W}}_{P1}$. Obviously, the optimal processing structure depends on knowledge of the source parameters $\boldsymbol{\theta}_n$, $n = 1,\ldots,3$. If these are unknown or changing, an adaptive method will be needed to track these and the processing changed accordingly from time to time.

## IV. ADAPTIVE SOURCE ENHANCEMENT AND TRACKING—1 SOURCE

Following the discussion in the last section, consider the tracking situation where the actual source parameters $\boldsymbol{\theta}_n$, $n = 1,\ldots,3$, are not known exactly, but some fairly good estimates $\hat{\boldsymbol{\theta}}_n$, $n = 1,\ldots,3$, of these are available from previous processing, and that these estimates have been used to design the structure of Fig. 2.

Denoting the differences of $\hat{\boldsymbol{\theta}}_n$, $n = 1,\ldots,3$, from their ideal values as

$$\delta\boldsymbol{\theta}_n = \boldsymbol{\theta}_n - \hat{\boldsymbol{\theta}}_n, \quad n = 1,\ldots,3 \tag{21}$$

and taking these to be small, the array input of (3) can be written in a first order approximation as

$$\mathbf{X}_t = \sum_{n=1}^{3} a_{nt}[\mathbf{S}(\hat{\boldsymbol{\theta}}_n) + \dot{\mathbf{S}}(\hat{\boldsymbol{\theta}}_n)\delta\boldsymbol{\theta}_n] + \mathbf{N}_t \tag{22}$$

where $\dot{\mathbf{S}}(\hat{\boldsymbol{\theta}}_n) \in C^{6\times 4}$ is the gradient of the space vector $\mathbf{S}(\hat{\boldsymbol{\theta}}_n)$ with respect to the parameter vector $\hat{\boldsymbol{\theta}}_n$, $n = 1,\ldots,3$:

$$\dot{\mathbf{S}}(\hat{\boldsymbol{\theta}}_n) = \begin{bmatrix} \dfrac{\partial\mathbf{S}(\hat{\boldsymbol{\theta}}_n)}{\partial\hat{\phi}_n} & \dfrac{\partial\mathbf{S}(\hat{\boldsymbol{\theta}}_n)}{\partial\hat{\psi}_n} & \dfrac{\partial\mathbf{S}(\hat{\boldsymbol{\theta}}_n)}{\partial\hat{\alpha}_n} & \dfrac{\partial\mathbf{S}(\hat{\boldsymbol{\theta}}_n)}{\partial\hat{\beta}_n} \end{bmatrix}$$
$$= \begin{bmatrix} \dfrac{\partial\mathbf{S}(\hat{\boldsymbol{\theta}}_n)}{\partial\hat{\boldsymbol{\theta}}_{n1}} & \dfrac{\partial\mathbf{S}(\hat{\boldsymbol{\theta}}_n)}{\partial\hat{\boldsymbol{\theta}}_{n2}} & \dfrac{\partial\mathbf{S}(\hat{\boldsymbol{\theta}}_n)}{\partial\hat{\boldsymbol{\theta}}_{n3}} & \dfrac{\partial\mathbf{S}(\hat{\boldsymbol{\theta}}_n)}{\partial\hat{\boldsymbol{\theta}}_{n4}} \end{bmatrix}. \tag{23}$$

The explicit form for this gradient with respect to the various parameters can be easily obtained by differentiation (2).

From (22), the first order approximation of the input covariance matrix is

$$\mathrm{E}[\mathbf{X}_t\mathbf{X}_t^{\mathrm{H}}] = \sum_{n=1}^{3}\sigma_n^2[\mathbf{S}(\hat{\boldsymbol{\theta}}_n)\mathbf{S}(\hat{\boldsymbol{\theta}}_n)^{\mathrm{H}} + \mathbf{S}(\hat{\boldsymbol{\theta}}_n)\delta\boldsymbol{\theta}_n^{\mathrm{H}}\dot{\mathbf{S}}(\hat{\boldsymbol{\theta}}_n)^{\mathrm{H}}$$
$$+ \dot{\mathbf{S}}(\hat{\boldsymbol{\theta}}_n)\delta\boldsymbol{\theta}_n\mathbf{S}(\hat{\boldsymbol{\theta}}_n)^{\mathrm{H}}] + \sigma^2\mathbf{I}_6. \tag{24}$$

As the design of the preprocessing $\mathbf{P}_1$ is actually based on $\hat{\boldsymbol{\theta}}_n$, $n = 1,\ldots,3$, in this tracking scenario, $\mathbf{P}_1$ will be orthogonal to $\mathbf{S}(\hat{\boldsymbol{\theta}}_2)$ and $\mathbf{S}(\hat{\boldsymbol{\theta}}_3)$, and

$$\mathbf{P}_1^{\mathrm{H}}\lfloor\mathbf{S}(\hat{\boldsymbol{\theta}}_2) \quad \mathbf{S}(\hat{\boldsymbol{\theta}}_3)\rfloor = 0. \tag{25}$$

Using (24), the first order approximation of the signal covariance matrix after preprocessing is then

$$\mathbf{R}_{11} = \mathrm{E}\lfloor\mathbf{X}_{1t}\mathbf{X}_{1t}^{\mathrm{H}}\rfloor = \mathrm{E}\lfloor\mathbf{P}_1^{\mathrm{H}}\mathbf{X}_t\mathbf{X}_t^{\mathrm{H}}\mathbf{P}_1\rfloor$$
$$= \sigma_1^2\mathbf{P}_1^{\mathrm{H}}[\mathbf{S}(\hat{\boldsymbol{\theta}}_1)\mathbf{S}(\hat{\boldsymbol{\theta}}_1)^{\mathrm{H}} + \mathbf{S}(\hat{\boldsymbol{\theta}}_1)\delta\boldsymbol{\theta}_1^{\mathrm{H}}\dot{\mathbf{S}}(\hat{\boldsymbol{\theta}}_1)^{\mathrm{H}}$$
$$+ \dot{\mathbf{S}}(\hat{\boldsymbol{\theta}}_1)\delta\boldsymbol{\theta}_1\mathbf{S}(\hat{\boldsymbol{\theta}}_1)^{\mathrm{H}}]\mathbf{P}_1 + \sigma^2\mathbf{L}_4$$
$$= \sigma_1^2\mathbf{P}_1^{\mathrm{H}}[\mathbf{S}(\hat{\boldsymbol{\theta}}_1) + \dot{\mathbf{S}}(\hat{\boldsymbol{\theta}}_1)\delta\boldsymbol{\theta}_1 I\mathbf{S}(\hat{\boldsymbol{\theta}}_1) + \dot{\mathbf{S}}(\hat{\boldsymbol{\theta}}_1)\delta\boldsymbol{\theta}_1]^{\mathrm{H}}\mathbf{P}_1$$
$$+ \sigma^2\mathbf{L}_4. \tag{26}$$

Equation (26) is interesting and useful as it shows that after preprocessing by $\mathbf{P}_1$, the signal vector $\mathbf{X}_{1t}$ has statistics which do not depend on $\delta\boldsymbol{\theta}_2$ and $\delta\boldsymbol{\theta}_3$. This is in spite of the fact that $\mathbf{P}_1$ is designed using $\hat{\boldsymbol{\theta}}_2$ and $\hat{\boldsymbol{\theta}}_3$, which are only estimates to the actual but unknown parameters $\boldsymbol{\theta}_2$ and $\boldsymbol{\theta}_3$.

The form of (26) serves as the basis through which the first source can be better tracked and from which $\boldsymbol{\theta}_1$ can be better estimated. Specifically, noting that (26) has the same form as (18), the weight vector $\tilde{\mathbf{W}}_{P1}$ that maximizes the SNR for this source is just proportional to

$$\tilde{\mathbf{W}}_{P1} \propto \mathbf{P}_1^{\mathrm{H}}\lfloor\mathbf{S}(\hat{\boldsymbol{\theta}}_1) + \dot{\mathbf{S}}(\hat{\boldsymbol{\theta}}_1)\delta\boldsymbol{\theta}_1\rfloor \tag{27}$$

which can be used to estimate $\delta\boldsymbol{\theta}_1$.

Following the above principle, Fig. 3 shows the processing structure adapted from Fig. 2 for adaptively receiving and locating the first source at maximum SNR while rejecting the other sources. The structure consists of the preprocessing $\mathbf{P}_1$ designed using previous estimates of the source parameters to remove the interfering sources. After preprocessing, the signal covariance matrix will be approximately given by (26) and will consist of contribution from the desired source and receiver noise. To receive this

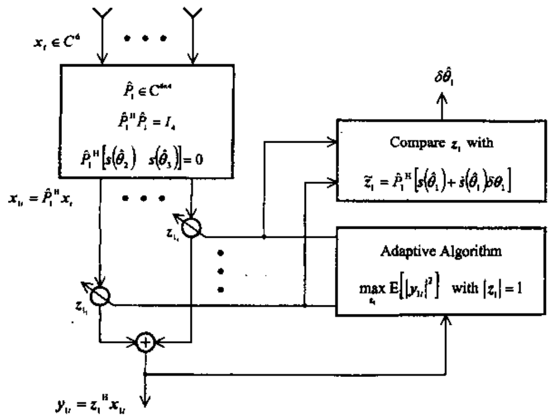


Fig. 3. Processing structure for adaptively receiving and locating the first source at maximum SNR while rejecting the other sources.

source as best as possible, an adaptive algorithm can be used to adjust the weight vector $\mathbf{W}_{P1}$ to maximize SNR. Since the choice of a unitary $\mathbf{P}_1$ has rendered the receiver noise to have a covariance of $\sigma^2\mathbf{I}_4$, the example algorithm chosen in Fig. 3 for maximizing SNR simply aims to

$$\max_{\mathbf{W}_{P1}} p_{y_1} = \min_{\mathbf{W}_{P1}} \mathrm{E}\lfloor |y_{1t}|^2 \rfloor \tag{28}$$

subject to the constraint

$$|\mathbf{W}_{P1}| = 1. \tag{29}$$

Other algorithms or objective functions that attempt to maximize SNR can also be used.

As $\mathbf{W}_{P1}$ approaches the optimal value for maximizing SNR, it can be compared with the theoretical value (27) obtained from the theoretical covariance matrix (26). As depicted in Fig. 3, this will lead to a better estimate of the desired signal location $\boldsymbol{\theta}_1$. To simplify this comparison process, the preprocessing $\mathbf{P}_1$ can be further chosen to satisfy

$$\mathbf{P}_1^{\mathrm{H}}\mathbf{S}(\hat{\boldsymbol{\theta}}_1) = [k_1 \quad 0 \quad 0 \quad 0]^{\mathrm{H}} \tag{30}$$

where $k_1$ is an appropriate constant. The Appendix shows how $\mathbf{P}_1$ can be designed using singular value decomposition to satisfy this and the other conditions given by (19) and (25). Applying (30), (27) becomes

$$\tilde{\mathbf{W}}_{P1} \propto \begin{bmatrix} 1 + \sum_{i=1}^{4} q_{1i}\delta\theta_{1i} \\ \sum_{i=1}^{4} q_{2i}\delta\theta_{1i} \\ \sum_{i=1}^{4} q_{3i}\delta\theta_{1i} \\ \sum_{i=1}^{4} q_{4i}\delta\theta_{1i} \end{bmatrix} = \begin{bmatrix} 1 \\ \sum_{i=1}^{4} q_{2i}\delta\theta_{1i} \\ \sum_{i=1}^{4} q_{3i}\delta\theta_{1i} \\ \sum_{i=1}^{4} q_{4i}\delta\theta_{1i} \end{bmatrix} \tag{31}$$

where the last result is a first order approximation and the constants in the summations are given by,

$$\begin{bmatrix} q_{11} & \cdots & q_{14} \\ \vdots & & \vdots \\ q_{41} & \cdots & q_{44} \end{bmatrix} = \mathbf{P}_1^{\mathrm{H}}\dot{\mathbf{S}}(\hat{\boldsymbol{\theta}}_1). \tag{32}$$

Normalizing with respect to the first element of $\tilde{\mathbf{W}}_{P1}$, an explicit equation that relates the unknown source parameter $\delta\boldsymbol{\theta}_1$ to elements of $\tilde{\mathbf{W}}_{P1}$ is

$$\begin{bmatrix} \mathrm{Re}\{[\tilde{\mathbf{W}}_{P1}]_2/[\tilde{\mathbf{W}}_{P1}]_1\} \\ \mathrm{Re}\{[\tilde{\mathbf{W}}_{P1}]_3/[\tilde{\mathbf{W}}_{P1}]_1\} \\ \mathrm{Re}\{[\tilde{\mathbf{W}}_{P1}]_4/[\tilde{\mathbf{W}}_{P1}]_1\} \\ \mathrm{Im}\{[\tilde{\mathbf{W}}_{P1}]_2/[\tilde{\mathbf{W}}_{P1}]_1\} \\ \mathrm{Im}\{[\tilde{\mathbf{W}}_{P1}]_3/[\tilde{\mathbf{W}}_{P1}]_1\} \\ \mathrm{Im}\{[\tilde{\mathbf{W}}_{P1}]_4/[\tilde{\mathbf{W}}_{P1}]_1\} \end{bmatrix} = \tilde{\mathbf{W}}_{P1R}$$

$$= \begin{bmatrix} \mathrm{Re}q_{21} & \mathrm{Re}q_{22} & \mathrm{Re}q_{23} & \mathrm{Re}q_{24} \\ \mathrm{Re}q_{31} & \mathrm{Re}q_{32} & \mathrm{Re}q_{33} & \mathrm{Re}q_{34} \\ \mathrm{Re}q_{41} & \mathrm{Re}q_{42} & \mathrm{Re}q_{43} & \mathrm{Re}q_{44} \\ \mathrm{Im}q_{21} & \mathrm{Im}q_{22} & \mathrm{Im}q_{23} & \mathrm{Im}q_{24} \\ \mathrm{Im}q_{31} & \mathrm{Im}q_{32} & \mathrm{Im}q_{33} & \mathrm{Im}q_{34} \\ \mathrm{Im}q_{41} & \mathrm{Im}q_{42} & \mathrm{Im}q_{43} & \mathrm{Im}q_{44} \end{bmatrix} \begin{bmatrix} \delta\theta_{11} \\ \delta\theta_{12} \\ \delta\theta_{13} \\ \delta\theta_{14} \end{bmatrix}$$

$$= \mathbf{Q}_{1R}\delta\boldsymbol{\theta}_1. \tag{33}$$

Note that (33) is written in real format to show that it corresponds to 6 real equations in 4 real unknowns. Clearly, under the tracking scenario of interest, the optimal $\tilde{\mathbf{W}}_{P1R}$ (from $\tilde{\mathbf{W}}_{P1}$) can be replaced by the corresponding $\mathbf{W}_{P1R}$ (from $\mathbf{W}_{P1}$) and the psuedoinverse of $\mathbf{Q}_{1R}$ used to obtain an estimate $\delta\hat{\boldsymbol{\theta}}_1$ of $\delta\boldsymbol{\theta}_1$:

$$\delta\hat{\boldsymbol{\theta}}_1 = \begin{bmatrix} \delta\hat{\theta}_{11} \\ \delta\hat{\theta}_{12} \\ \delta\hat{\theta}_{13} \\ \delta\hat{\theta}_{14} \end{bmatrix} = \begin{bmatrix} \delta\hat{\phi}_1 \\ \delta\hat{\psi}_1 \\ \delta\hat{\alpha}_1 \\ \delta\hat{\beta}_1 \end{bmatrix} = \mathbf{Q}_{1R}^{+}\mathbf{W}_{P1R}$$

$$= \mathbf{Q}_{1R}^{+} \begin{bmatrix} \mathrm{Re}\{[\mathbf{W}_{P1}]_2/[\mathbf{W}_{P1}]_1\} \\ \mathrm{Re}\{[\mathbf{W}_{P1}]_3/[\mathbf{W}_{P1}]_1\} \\ \mathrm{Re}\{[\mathbf{W}_{P1}]_4/[\mathbf{W}_{P1}]_1\} \\ \mathrm{Im}\{[\mathbf{W}_{P1}]_2/[\mathbf{W}_{P1}]_1\} \\ \mathrm{Im}\{[\mathbf{W}_{P1}]_3/[\mathbf{W}_{P1}]_1\} \\ \mathrm{Im}\{[\mathbf{W}_{P1}]_4/[\mathbf{W}_{P1}]_1\} \end{bmatrix} \tag{34}$$

where

$$\mathbf{Q}_{1R}^{+} = (\mathbf{Q}_{1R}^{\mathrm{T}}\mathbf{Q}_{1R})^{-1}\mathbf{Q}_{1R}^{\mathrm{T}}. \tag{35}$$

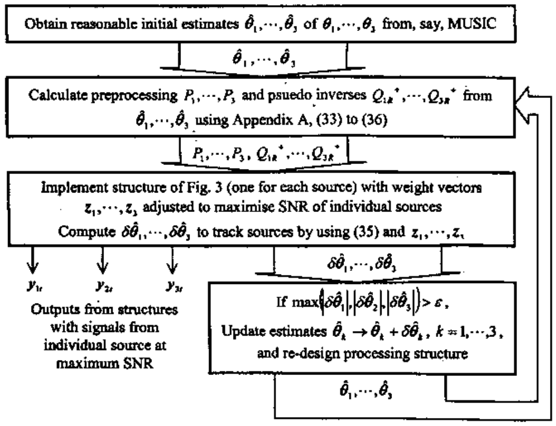


Fig. 4. Processing structure for adaptively receiving and tracking all sources at maximum SNR.

## V. ADAPTIVE SOURCE ENHANCEMENT AND TRACKING—ALL SOURCES

As described, under a tracking scenario where the latest estimates $\hat{\theta}_n$, $n = 1,\ldots,3$, of the sources are available, the structure of Fig. 3 has the capability to adaptively enhance source $\theta_1$ for maximum SNR, while rejecting the other 2 sources $\theta_2$ and $\theta_3$. Also, by using (34) and (35), a better estimate $\hat{\theta}_1 + \delta\hat{\theta}_1$ of $\theta_1$ can be obtained from the adaptive weight vector $\mathbf{W}_{P1}$ used for enhancing source $\theta_1$. The same structure and procedure can be used for sources $\theta_2$ and $\theta_3$, with the result that these 2 will also be adaptively enhanced for maximum SNR and, at the same time, better estimates $\hat{\theta}_2 + \delta\hat{\theta}_2$ and $\hat{\theta}_3 + \delta\hat{\theta}_3$ for the other sources $\theta_2$ and $\theta_3$ can be obtained.

The structure on which these are based comes from the first order approximation of (22) which will be valid if $\delta\theta_n = \theta_n - \hat{\theta}_n$, $n = 1,\ldots,3$, is small. Specifically, the crucial preprocessing $\mathbf{P}_1$ of Fig. 3 is designed based on $\hat{\theta}_n$, $n = 1,\ldots,3$, and will function well if $\delta\theta_n$, $n = 1,\ldots,3$, is small. With $\delta\hat{\theta}_n$ providing an estimate to $\delta\theta_n$, $n = 1,\ldots,3$, it is easy to find out if the first order approximation is likely to be valid. For example, when any of the estimated $\delta\hat{\theta}_n$, $n = 1,\ldots,3$, is found to have magnitude that exceeds a certain threshold $\varepsilon$ or

$$\max(|\delta\hat{\theta}_1|,|\delta\hat{\theta}_2|,|\delta\hat{\theta}_3|) > \varepsilon \qquad (36)$$

the preprocessing can be taken to have exceeded its limit of operation and a redesign is initiated. This redesign can be based on

$$\hat{\theta}_n \to \hat{\theta}_n + \delta\hat{\theta}_n, \qquad n = 1,\ldots,3 \qquad (37)$$

which will give better estimates to $\theta_n$, $n = 1,\ldots,3$, and will "realign" the preprocessing to better fit the latest environment. Fig. 4 gives a block diagram of the process involved.

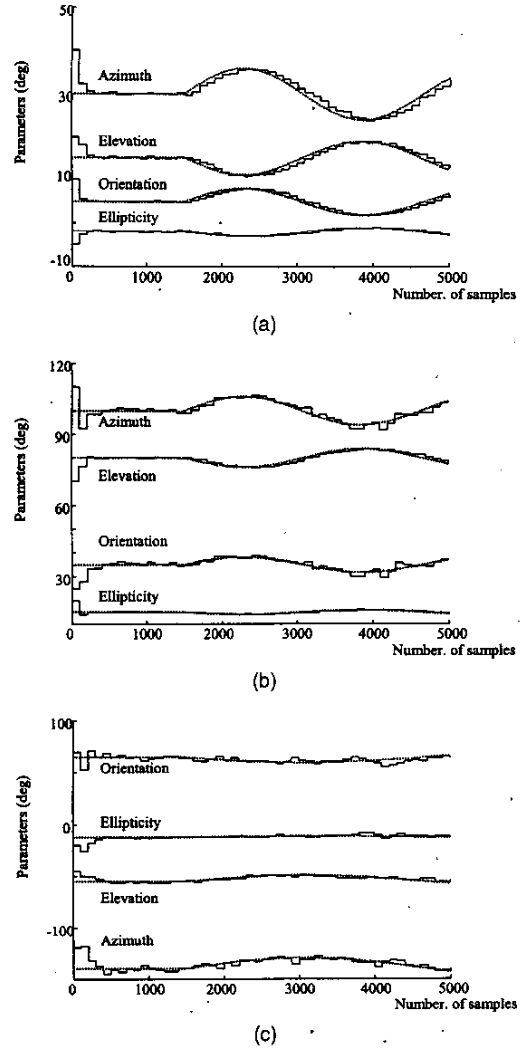


Fig. 5. Source parameter trajectories under scenario when Source 1 and 2 have the same 30 dB power and Source 3 has 20 dB power. Dotted lines give actual parameters and solid lines are from new algorithm. (a) Source 1. (b) Source 2. (c) Source 3.

## VI. SIMULATION RESULTS

Some simulation results are now presented to illustrate the tracking capability of the algorithm. The environment consists of three uncorrelated broadband sources with powers 30, 30, and 20 dB, and initial parameters $\theta_1 = [\phi_1,\varphi_1,\alpha_1,\beta_1]^T = [30°,15°,5°,-2°]^T$, $\theta_2 = [100°,80°,35°,15°]^T$, and $\theta_3 = [-140°,-55°,65°,-12°]^T$ in the presence of 0 dB receiver noise. These parameters are changed in a manner as shown by the dotted lines in Fig. 5, which also shows the trajectories of the parameters as estimated by the proposed algorithm. The initial parameters used in the algorithm are $\hat{\theta}_1 = [40°,20°,-10°,-5°]^T$, $\hat{\theta}_2 = [110°,70°,25°,20°]^T$, and $\hat{\theta}_3 = [-120°,-45°,70°,-10°]^T$, and these can be obtained by, say, the standard MUSIC algorithm before using the new algorithm for tracking purposes.

The updating of the weight vector and preprocessor for maximizing SNR and source separation is carried out periodically once every 100 data samples based on the sample covariance matrix obtained from the last 100 data samples. Also, the optimal weight vector for maximizing SNR is calculated from finding the principal eigenvector (associated with the largest eigenvalue) of the sample covariance matrix. Note that for a covariance matrix with a form given by (26), the principal eigenvector is the solution of the problem given by (28) and (29). Clearly, even though some of the initial estimates used in the algorithm are not really closed to the actual source parameters, the results given by Fig. 5 shows that the proposed algorithm is able to separate out the sources and track them well.

Fig. 6 compares the performance of the new algorithm with the cross-product algorithm proposed in [6]. The latter is based on finding the cross-product of the electric and magnetic field component vectors in the output vector of the EMVS. The cross-product of these two component vectors corresponds to the Poynting vector of electromagnetic wave propagation and can be used to give the azimuth and elevation of the source signal arriving at the EMVS.

Since the cross-product algorithm is able to estimate the direction of only one source, the environment used consists of a 20 dB source with initial parameter $\boldsymbol{\theta}_1 = [\phi_1, \varphi_1, \alpha_1, \beta_1]^{\mathrm{T}} = [30°, 50°, -60°, 15°]^{\mathrm{T}}$ in the presence of 0 dB receiver noise. The values of $\phi_1$ and $\varphi_1$ are changed as shown by the dashed lines in Fig. 6. The solid and dotted lines show the behavior of the new and cross-product algorithms, respectively. For both the new and the cross-product algorithms, the parameters are updated once every 100 data samples based on the sample covariance matrix from the previous 100 data samples.

In the steady state after initial convergence and before $\phi_1$ and $\varphi_1$ change, the two algorithms have almost the same root mean square angular errors of about 0.6°. During the period when $\phi_1$ and $\varphi_1$ are changing in a sinusoidal manner, the average lags in azimuth are found to be 1.45° for the new algorithm and 1.49° for the cross product algorithm, while the average lags in elevation for them are 0.61° and 0.54°, respectively. This shows that, besides having the ability to acquire polarization parameters and identifying up to three sources simultaneously, the new algorithm has the same DOA tracking ability as the cross-product algorithm when one source is present.

In terms of computational complexity, the cross-product algorithm requires 6 multiplications per sample for calculating the cross product for the purpose of tracking 1 source. On the other hand, the new algorithm requires forming the sample covariance matrix, calculating the preprocessing matrix, and carrying out an eigen-decompositon together with

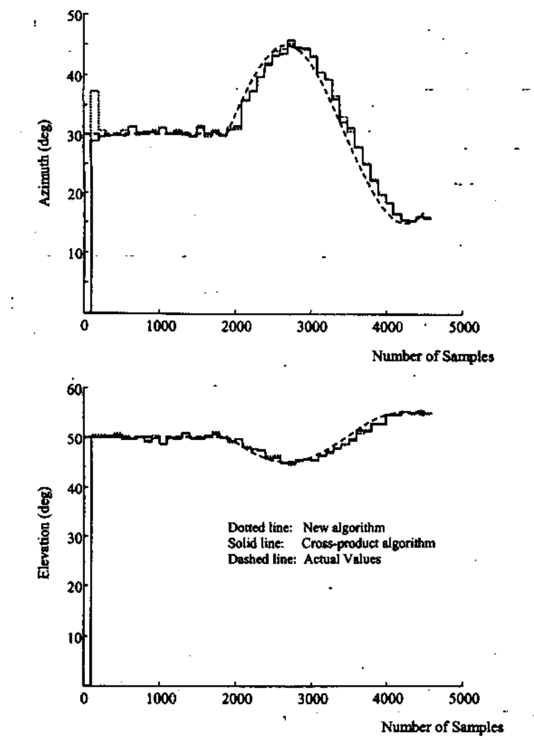


Fig. 6. Comparison of new algorithm with cross-product algorithm.

other auxiliary equations every time a new update to the source parameters has to be calculated. With the size of the matrix involved being 6, a detailed trace of the computational tasks show that this involves a total of about $1000 + 18N$ multiplications per update, where $N$ is the number of samples per update. The value of $18N$ is for the formation of the hermetian sample covariance matrix, while the value of 1000 is for the other tasks which have to be done once per update. For the environment of Fig. 6 where $N$ is 100, the new algorithm requires about 28 multiplications per update. Clearly, the new algorithm has a complexity that is higher than the cross-product algorithm, but not excessive after taking into consideration that it has the capability to track 2 more sources.

## VII. CONCLUSIONS

This paper has proposed a new structure for adaptively separating, enhancing and tracking uncorrelated sources using an EMVS. The structure consists of a set of parallel spatial processors for tracking source individually, with two stages of processing in each spatial processor. The first preprocessing stage rejects all other sources except the one of interest, while the second stage is an adaptive one for maximising the SNR and tracking the desired source. The preprocessings are designed using the latest source parameter estimates obtained from the source trackers, and a redesign is activated periodically or whenever any source has been detected by the source trackers to have made significant movement. Compared with conventional adaptive beamforming, the algorithm has the advantage that no a priori information on any desired signal location is needed, the sources are separated at maximum SNR, and their locations are available. The structure is also well suited for parallel implementation.

## APPENDIX. DESIGN OF PREPROCESSING

Without loss of generality, consider the design of the preprocessing $\mathbf{P}_1 \in C^{6\times4}$. From the main text, this has to satisfy

$$\mathbf{P}_1^{\mathrm{H}}[\mathbf{S}(\hat{\theta}_1) \quad \mathbf{S}(\hat{\theta}_2) \quad \mathbf{S}(\hat{\theta}_3)] = \begin{bmatrix} k_1 & 0 & 0 \\ 0 & 0 & 0 \\ 0 & 0 & 0 \\ 0 & 0 & 0 \end{bmatrix} \tag{38}$$

and

$$\mathbf{P}_1^{\mathrm{H}}\mathbf{P}_1 = \mathbf{I}_4 \tag{39}$$

where $k_1$ is an appropriate constant.

Using singular value decomposition, $[\mathbf{S}(\hat{\theta}_1) \ \mathbf{S}(\hat{\theta}_2) \ \mathbf{S}(\hat{\theta}_3)] \in C^{6\times3}$ can be decomposed as

$$[\mathbf{S}(\hat{\theta}_1) \quad \mathbf{S}(\hat{\theta}_2) \quad \mathbf{S}(\hat{\theta}_3)] = \mathbf{U} \begin{bmatrix} \lambda_1 & 0 & 0 \\ 0 & \lambda_2 & 0 \\ 0 & 0 & \lambda_3 \\ 0 & 0 & 0 \\ 0 & 0 & 0 \\ 0 & 0 & 0 \end{bmatrix} \mathbf{V}^{\mathrm{H}} \tag{40}$$

where both $\mathbf{U} \in C^{6\times6}$ and $\mathbf{V} \in C^{3\times3}$ are unitary:

$$\mathbf{U}^{\mathrm{H}}\mathbf{U} = \mathbf{I}_6 \tag{41}$$

and

$$\mathbf{V}^{\mathrm{H}}\mathbf{V} = \mathbf{I}_3. \tag{42}$$

Substituting (40) and using (41), (38) becomes

$$\mathbf{P}_1^{\mathrm{H}}\mathbf{U} \begin{bmatrix} \lambda_1 & 0 & 0 \\ 0 & \lambda_2 & 0 \\ 0 & 0 & \lambda_3 \\ 0 & 0 & 0 \\ 0 & 0 & 0 \\ 0 & 0 & 0 \end{bmatrix} = \begin{bmatrix} k_1 & 0 & 0 \\ 0 & 0 & 0 \\ 0 & 0 & 0 \\ 0 & 0 & 0 \end{bmatrix} \mathbf{V} = \begin{bmatrix} [\mathbf{V}]_{11} & [\mathbf{V}]_{12} & [\mathbf{V}]_{13} \\ 0 & 0 & 0 \\ 0 & 0 & 0 \\ 0 & 0 & 0 \end{bmatrix} \tag{43}$$

The general solution of (43) is

$$\mathbf{P}_1^{\mathrm{H}}\mathbf{U} = \begin{bmatrix} k_1\lambda_1^{-1}[\mathbf{V}]_{11} & k_1\lambda_2^{-1}[\mathbf{V}]_{12} & k_1\lambda_3^{-1}[\mathbf{V}]_{13} & \\ 0 & 0 & 0 & \\ 0 & 0 & 0 & \\ 0 & 0 & 0 & \mathbf{H} \in C^{4\times3} \end{bmatrix} \tag{44}$$

where $\mathbf{H}$ is any arbitrary $4 \times 3$ matrix. Obviously, the design of $\mathbf{P}_1$ will be complete by choosing $\mathbf{H}$ so that (39) is satisfied.

Using (41), (44) leads to

$$\mathbf{P}_1^{\mathrm{H}}\mathbf{U}\mathbf{U}^{\mathrm{H}}\mathbf{P}_1 = \mathbf{P}_1^{\mathrm{H}}\mathbf{P}_1 = \sum_{i=1}^{3} \left| \frac{k_1[\mathbf{V}]_{1i}}{\lambda_i} \right|^2 \begin{bmatrix} 1 \\ 0 \\ 0 \\ 0 \end{bmatrix} \begin{bmatrix} 1 \\ 0 \\ 0 \\ 0 \end{bmatrix}^{\mathrm{H}} + \mathbf{H}\mathbf{H}^{\mathrm{H}}. \tag{45}$$

Equating this to (39), $\mathbf{H}$ has to satisfy

$$\mathbf{H}\mathbf{H}^{\mathrm{H}} = \mathbf{I}_4 - \sum_{i=1}^{3} \left| \frac{k_1[\mathbf{V}]_{1i}}{\lambda_i} \right|^2 \begin{bmatrix} 1 \\ 0 \\ 0 \\ 0 \end{bmatrix} \begin{bmatrix} 1 \\ 0 \\ 0 \\ 0 \end{bmatrix}^{\mathrm{H}}. \tag{46}$$

Since the rank of $\mathbf{H} \in C^{4\times3}$ is 3 whereas the rank of $\mathbf{I}_4$ is 4, (46) can be satisflied if $k_1$ is chosen to be

$$\sum_{i=1}^{3} \left| \frac{k_1[\mathbf{V}]_{1i}}{\lambda_i} \right|^2 = 1. \tag{47}$$

With $k_1$ satisfying this, (46) becomes simply

$$\mathbf{H}\mathbf{H}^{\mathrm{H}} = \begin{bmatrix} 0 & 0 & 0 & 0 \\ 0 & 1 & 0 & 0 \\ 0 & 0 & 1 & 0 \\ 0 & 0 & 0 & 1 \end{bmatrix}. \tag{48}$$

The solution of this is

$$\mathbf{H} = \begin{bmatrix} 0 \quad 0 \quad 0 \\ \mathbf{H}_U \in C^{3\times3} \end{bmatrix} \tag{49}$$

where $\mathbf{H}_U$ is any unitary $3 \times 3$ matrix:

$$\mathbf{H}_U^{\mathrm{H}}\mathbf{H}_U = \mathbf{I}_3. \tag{50}$$

Combining the relevant equations, the preprocessing $\mathbf{P}_1$ that satisfies (38) and (39) is given by

$$\mathbf{P}_1^{\mathrm{H}} = \begin{bmatrix} k_1\lambda_1^{-1}[\mathbf{V}]_{11} & k_1\lambda_2^{-1}[\mathbf{V}]_{12} & k_1\lambda_3^{-1}[\mathbf{V}]_{13} & 0 \quad 0 \quad 0 \\ 0 & 0 & 0 & \\ 0 & 0 & 0 & \mathbf{H}_U \\ 0 & 0 & 0 & \end{bmatrix} \mathbf{U}^{\mathrm{H}} \tag{51}$$

where $k_1$ is given by (47) and $\mathbf{H}_U$ is any unitary $3 \times 3$ matrix.

C. C. KO
J. ZHANG
Department of Electrical and Computer Engineering
National University of Singapore
Block E4, Level 5, Rm. 48
4 Engineering Drive 3
Singapore 0511
E-mail: (elekocc@nus.edu.sg)

A. NEHORAI
Department of Electrical Engineering and Computer Systems
University of Illinois at Chicago
Chicago, IL

REFERENCES

[1] Nehorai, A., and Paldi, E. (1991)
Vector-sensor array processing for electromagnetic source localization.
In *Proceedings of the 25th Asilomar Conference Signals, Systems Computers*, Nov. 1991, 566–572.

[2] Nehorai, A., and Paldi, E. (1994)
Vector-sensor array processing for electromagnetic source localization.
*IEEE Transactions on Signal Processing*, **42** (1994), 376–398.

[3] Tan, K. C., Ho, K. C., and Nehorai, A. (1996)
Linear independence of steering vectors of an electromagnetic vector sensor.
*IEEE Transactions on Signal Processing*, **44** (1996), 3099–3107.

[4] Hochwald, B., and Nehorai, A. (1996)
Identifiability in array processing models with vector-sensor applications.
*IEEE Transactions on Signal Processing*, **44** (Jan. 1996), 83–95.

[5] Nehorai, A., Ho, K. C., and Tan, B. T. G. (1999)
Minimum-noise-variance beamformer with an electromagnetic vector sensor.
*IEEE Transactions on Signal Processing*, **47** (1999), 601–618.

[6] Nehorai, A., and Tichavsky, P. (1999)
Cross-product algorithms for source tracking using an EM vector sensor.
*IEEE Transactions on Signal Processing*, **47** (1999), 2863–2867.

[7] Hatke, G. F. (1992)
Performance analysis of the superCART antenna array.
Project Report AST-22, MIT Lincoln Lab, 1992.

[8] Hirari, M., and Hayahawa, M. (1997)
DOA estimation using blind separation of sources.
In *Proceedings of the IEEE Signal Processing Workshop on Higher-Order Statistics* (1997), 311–315.

[9] Ho, K. C., Tan, K. C., and Nehorai, A. (1999)
Estimating directions of arrival of completely and incompletely polarized signals with electromagnetic vector sensors.
*IEEE Transactions on Signal Processing*, **47**, 10 (Oct. 1999), 2845–2849.

[10] Li, J. (1993)
Direction and polarization estimation using arrays with small loops and short dipoles.
*IEEE Transactions on Antennas Propagation*, **41**, 2 (Mar. 1993), 379–387.

[11] Wong, K. T., and Zoltowski, M. D. (1997)
Uni-vector-sensor ESPRIT for multisource azimuth, elevation and polarization estimation.
*IEEE Transactions on Antennas and Propagation*, **45**, 10 (Oct. 1997), 1467–1474.

[12] Wong, K. T., and Zoltowski, M. D. (2000)
ESPRIT-based 2D direction finding with a sparse array of electromagnetic vector-sensors.
*IEEE Transactions on Signal Processing* (Aug. 2000), 2195–2204.

[13] Wong, K. T., and Zoltowski, M. D. (2000)
Closed-form direction-finding with arbitrarily spaced electromagnetic vector-sensors at unknown locations.
*IEEE Transactions on Antennas and Propagation* (May 2000), 671–681.

[14] Wong, K. T., and Zoltowski, M. D. (2000)
Self-initiating MUSIC-based direction finding and polarization estimation in spatio-polarizational beamspace.
*IEEE Transactions on Antennas and Propagation* (Sept. 2000), 1235–1245.

[15] Ko, C. C. (1999)
Two-dimensional adaptive array for spatially separating and tracking uncorrelated sources.
*IEEE Transactions on Aerospace and Electronic Systems*, **35** (1999), 93–101.

## Horizontal Waypoint Guidance Design Using Optimal Control

**A horizontal waypoint guidance algorithm is proposed by applying line-following guidance to waypoint line segments in sequence. The line-following guidance is designed using an LQR (linear quadratic regulator). Then, the optimal waypoint changing points are derived by minimizing the accelerations required for changing the waypoint line segments. Also derived is a sufficient condition for the stability bound of ground speed changes based on the Lyapunov Stability Theorem. Simulation results show that the proposed algorithm can effectively guide a vehicle along the sequence of waypoint line segments.**

### I. INTRODUCTION

A general way to make an unmanned vehicle fly along a trajectory is to design the guidance algorithms in the horizontal and vertical planes separately. In this case, the horizontal guidance is often designed for threat avoidance, terrain masking, achievement of desired attack directions, or arrival at the target location at a desired time, while the vertical guidance

Manuscript received June 23, 1999; released for publication June 24, 2002.

IEEE Log No. T-AES/38/3/XXXX.

Refereeing of this contribution was handled by T. F. Roome.

0018-9251/02/$17.00 